Oscillatory dynamics in nanocavities with noninstantaneous Kerr response

Andrea Armaroli,* Stefania Malaguti, Gaetano Bellanca, and Stefano Trillo
Department of Engineering, University of Ferrara, Via Saragat 1, IT 44122 Ferrara, Italy

Alfredo de Rossi and Sylvain Combrié
Thales Research and Technology, Palaiseau Cedex FR 91767, France
(Received 3 July 2011; published 9 November 2011)

We investigate the impact of a finite response time of Kerr nonlinearities over the onset of spontaneous oscillations (self-pulsing) occurring in a nanocavity. The complete characterization of the underlying Hopf bifurcation in the full parameter space allows us to show the existence of a critical value of the response time and to envisage different regimes of competition with bistability. The transition from a stable oscillatory state to chaos is found to occur only in cavities which are detuned far off-resonance, which turns out to be mutually exclusive with the region where the cavity can operate as a bistable switch.

DOI: 10.1103/PhysRevA.84.053816 PACS number(s): 42.65.Pc, 42.65.Sf, 42.55.Sa

I. INTRODUCTION

Self-pulsing (SP), the onset of spontaneous oscillations, is a universal feature of nonlinear structures with feedback. As long as passive systems are concerned SP has been investigated theoretically in settings ranging from isolated ring cavities [1–3] and parametric intracavity mixing [4–6] to Bragg gratings [7,8] or grating-assisted backward frequency conversion schemes [9,10], and it is still a subject of active research [11–13]. In particular, the dynamics of nonlinear passive cavities, whose study was pioneered in the 1980s [1–3], is extremely rich, encompassing stable as well as chaotic SP which can compete with bistabilities and transverse effects [14]. Historically, SP and chaos (the optical equivalent of strong turbulence) have been first analyzed by means of delay-differential models accounting for the round-trip delay at each passage, which can be large in ring cavities. An instability named after Ikeda occurs in this framework when the relaxation time of the nonlinear response is much shorter than the transit time [1] and has been tested experimentally [15]. However SP and so-called weak turbulence occur also in the opposite (say, *short cavity*) limit, where the delay can be averaged out to end up with a differential mean-field model [2]. This regime becomes important nowadays where nanocavities are employed for many modern photonic applications [16], including bistability [17], demonstrated in photonic crystal (PhC) membranes which offer great flexibility of design as well as high nonlinear performances in semiconductors [18–25]. In these cavities, transverse effects are absent and their dimensions are so small that the response time of the medium can be much larger than the light transit time in the cavity yet comparable to the photon lifetime, which is strongly enhanced on account of the large quality factor Q. SP in such nanocavities has been recently predicted, owing to the free-carrier dispersion induced by two-photon absorption [13]. The main feature of such a mechanism is the existence of a critical value of the time relaxation constant τ, as well as a wide region of the parameter space where stable (nonchaotic) SP can be potentially observed. In this paper we analyze the dynamics of a nanoresonator in the good-cavity limit when the underlying nonlinear mechanism is a Kerr-like nonlinearity with finite response time. Our analysis is based on the differential model proposed in Ref. [2]. In spite of the simplicity of such a model, which makes it an ideal prototype for understanding the role of relaxation processes, a full characterization of SP and its competition with bistability in the full parameter space was never reported (to the best of our knowledge) after Ref. [2]. We propose such an analysis, adopting a different normalization with respect to that employed in Ref. [2], better aimed at capturing the key role of the relaxation time. This is especially important nowadays in view of assessing how a given designed nanocavity may be expected to behave by changing the characteristic relaxation time of the nonlinearity as a consequence of choosing different materials and/or adopting techniques for fine-tuning their response time. We propose an analytical characterization of the SP instability and its competition with bistability in the full parameter space, pointing out the qualitative similarity with the features observed for a nonlinearity dominated by free-carrier dispersion [13]. Nonetheless, we further investigate also the destabilization mechanism of the oscillatory states initially described in Ref. [2], showing that the chaotic regime, being confined to far off-resonance cavities, is indeed mutually exclusive with bistable switching.

II. MODEL DEFINITION AND LINEAR STABILITY ANALYSIS

We start from the following dimensionless coupled-mode model that rules the temporal evolution of the normalized intracavity field $a(t)$ coupled to the frequency deviation $n(t)$, owing to the intensity-dependent refractive index change:

$$\frac{da}{dt} = \sqrt{P} + i(\delta + \chi n)a - a, \tag{1a}$$

$$\tau \frac{dn}{dt} + n = |a|^2. \tag{1b}$$

Noteworthy, Eqs. (1) describe a photonic crystal nanocavity with high Q coupled to a line-defect waveguide [18,20,24] and implicitly assume that the nonlinearity is dominated solely by the Kerr effect with relaxation time τ, while other possible

*andrea.armaroli@unife.it

nonlinear contributions, e.g., two-photon absorption along with the free-carrier dispersion [13,18,20,24], are neglected. Here P is the normalized power injected in the cavity through coupling with the waveguide, and $|a|^2$ is the normalized intracavity energy, which can be easily rescaled into real-world units by comparison with widely used dimensional models (see, e.g., [24]). It is worth emphasizing that a unit coefficient in front of the loss term in Eqs. (1) implies that the time t is measured in units of the inverse damping coefficient $1/\Gamma_0 = 2Q/\omega_0 = 2t_c$, where Q, ω_0, and t_c stand for the overall quality factor, the resonant frequency, and the photon lifetime of the cavity, respectively. In these units, the two key (normalized) parameters are the detuning $\delta = (\omega_0 - \omega)/\Gamma_0$ and the time constant $\tau = \tau_p \Gamma_0$, where τ_p is the response time of the nonlinearity in real-world units, while $\chi = \pm 1$ accounts for the sign of the nonlinear Kerr coefficient. We point out that our model differs from Ref. [2], inasmuch as the time scale is referred to the cavity lifetime instead of the response time of the medium. Indeed Eqs. (1) can be reduced to the model analyzed in Ref. [2] by means of the substitution $a,n,t \to a/\sqrt{\tau}, n/\tau, \tau t$. The effect of such a transformation is however to rescale the detuning and the injected power in such a way that they become dependent on the response time of the medium, which is not suitable for our purpose of investigating the impact of the relaxation time on the dynamics of a given cavity with fixed characteristics.

For a cw driving $P = \text{const}$, Eqs. (1) have the steady-state solution $a(t) = A$, $n(t) = N = |A|^2$, where

$$P = E[1 + (\delta + \chi E)^2], \tag{2}$$

$E = |A|^2$ being the stationary intracavity energy. It is well known that bistability occurs for $\delta > \sqrt{3}$ when $\chi = -1$, and $\delta < -\sqrt{3}$ when $\chi = 1$ [14]. In the discussion below, we will focus on the latter case, where the cavity resonance is blue-shifted due to the nonlinearity, a case which is directly comparable to the net effect of free-carrier dispersion induced by two-photon absorption [13]. All the conclusions of this paper remain valid also for $\chi = -1$, provided $\delta \to -\delta$. The values of intracavity energies corresponding to the knees of the bistable response are

$$E_b^{\pm} = \frac{-2\chi\delta \pm \sqrt{\delta^2 - 3}}{3}, \tag{3}$$

and the corresponding input powers $P_b^{\pm} = P(E_b^{\pm})$ can be calculated by means of Eq. (2).

The stability of solution (2) can be investigated by plugging into Eqs. (1) the ansatz $a(t) = A + \delta a(t)$, $n(t) = N + \delta n(t)$, while retaining linear terms in the perturbations $\delta a, \delta n$.

The perturbation column array $\varepsilon \equiv (\delta a, \delta a^*, \delta n)^T$ is found to obey the following linearized equation:

$$\frac{d\varepsilon}{dt} = M\varepsilon, \tag{4a}$$

$$M = \begin{pmatrix} i\hat{\delta} - 1 & 0 & i\chi A \\ 0 & -i\hat{\delta} - 1 & -i\chi A^* \\ A^*/\tau & A/\tau & -1/\tau \end{pmatrix}, \tag{4b}$$

where $\hat{\delta} \equiv \delta + \chi E$.

The characteristic equation of M reads as

$$\lambda^3 + a_2\lambda^2 + a_1\lambda + a_0 = 0, \tag{5}$$

where the coefficients are $a_2 = 2 + \frac{1}{\tau}$, $a_1 = (1 + \hat{\delta}^2 + \frac{2}{\tau})$, and $a_0 = \frac{1}{\tau}(1 + \hat{\delta}^2 + 2\chi E\hat{\delta})$.

SP occurs when the system undergoes a Hopf bifurcation, i.e., a pair of complex-conjugate eigenvalues $\lambda_R \pm i\lambda_I$ crosses into the right-half complex plane, entailing an exponential growth of a pulsating perturbation with period $T = 2\pi/|\lambda_I|$. The bifurcation point ($\lambda_R = 0$) corresponds to the constraint $a_1 a_2 = a_0$, which can be solved to yield the following explicit expression for the SP (Hopf) threshold values $E_H^{\pm}$:

$$E_H^{\pm} = \frac{-\chi\delta\left(2 - \frac{1}{\tau}\right) \pm \sqrt{\frac{\delta^2}{\tau^2} - 4\left(1 + \frac{1}{\tau}\right)^2\left(1 - \frac{1}{\tau}\right)}}{2\left(1 - \frac{1}{\tau}\right)}, \tag{6}$$

and the corresponding injected power threshold $P_H^{\pm} = E_H^{\pm}[1 + (\delta + \chi E_H^{\pm})^2]$.

The analysis reported above shows that the bistable response depends only on the detuning, while the time constant τ can affect qualitatively the onset of SP due to the Hopf bifurcation. In fact different scenarios are possible depending on the existence of one or both Hopf thresholds [in turn corresponding to the roots in Eq. (6) being real and positive], and whether they occur at powers above or below the bistable knee for up-switching. Four possible scenarios are displayed in Fig. 1, where we show the bistable stationary response along with the unstable eigenvalues responsible for instabilities. First, Fig. 1 shows the well-known fact that a purely real and positive eigenvalue of M leads to instability of the steady-state solution along the negative slope branch, which turns out to be a saddle point in phase space. Conversely, SP is characterized by a pair of complex-conjugate eigenvalues, and the relative thresholds are highlighted by empty triangles. We find such a threshold to occur always on the upper branch of the bistable response (or when the response is monotone; see below). However, depending on the value of τ, the lower Hopf threshold $P(E_H^-)$ can take place above [as in Figs. 1(a) and 1(c)] or below [see Figs. 1(b) and 1(d)] the knee $P(E_b^-)$, which characterizes the bistable up-switching. In the former case the cavity can exhibit bistable up-switching to a stable steady state, whereas in the latter case up-switching occurs inevitably toward a SP-unstable state: stabilization is achieved by moving along the hysteresis cycle below the Hopf threshold. Moreover, also depending on the value of τ, the upper branch can be indefinitely SP-unstable above the first threshold $P(E_H^-)$ [see Figs. 1(a) and 1(b)] or, vice versa, can exhibit a SP switch-off energy or secondary threshold beyond which SP ceases to take place [see Figs. 1(c) and 1(d); note that we change the detuning in Fig. 1(d) only to make the picture clearer, though the same qualitative behavior occurs at $\delta = -4$]. Indeed, if $\tau \geqslant 1$, Eq. (6) may also admit a real solution E_H^+, and hence SP occurs only in a finite range of energies (and powers) $E_H^- < E < E_H^+$. When τ grows, this finite interval shrinks and vanishes as a critical value $\tau = \tau_c$ is reached. For $\tau = \tau_c$, SP no longer takes place and the entire upper branch becomes stable. From Eq. (6), we find such a critical value τ_c to be

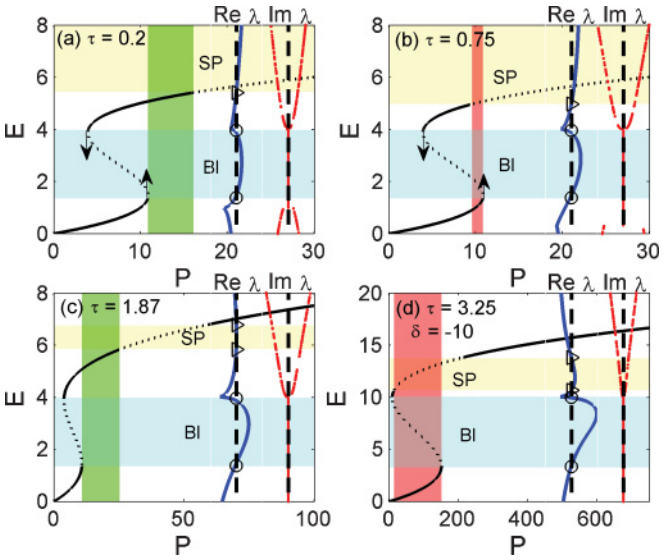

FIG. 1. (Color online) Steady-state response E vs P for (a)–(c) $\delta = -4$ and (d) $\delta = -10$ and different τ ($\chi = 1$). Stable and unstable branches are reported as solid and dotted lines, respectively. The blue and red curves superimposed on the right side show how the real part Re(λ) and imaginary part Im(λ) (of the dominant eigenvalue underlying the instability) change with E. Bifurcation points are highlighted over with the dashed line Re(λ) = 0. The shaded regions labeled BI (light blue) and SP (light yellow) correspond to the negative slope branch of the bistable response (real eigenvalue) and SP instability (pair of conjugate eigenvalues with a positive real part), respectively. Four different scenarios are shown: (a) SP occurs at $P = P_H^-$ values above the bistable knee value P_b^- and is unbounded for increasing P; (b) SP occurs at $P = P_H^-$ values below the bistable knee P_b^-, still being unbounded; (c) as in (a), except SP occurs in a finite range below a given value $P = P_H^+$; and (d) as in (b), except SP occurs in a finite range below a given value $P = P_H^+$. The shaded green regions yield the range of power where bistable up-switching to a stable state is permitted, while red ones identify the coexistence of a SP and an unstable saddle branch.

given by the positive real root of the cubic polynomial (its explicit expression is too cumbersome):

$$\tau_c^3 + \tau_c^2 - \left(1 + \frac{\delta^2}{4}\right)\tau_c - 1 = 0, \quad \tau_c \approx \frac{|\delta|}{2}, \quad |\delta| \gg 1. \tag{7}$$

The behavior discussed above can be clearly seen by reporting the SP threshold energies $E_H^{\pm}$ versus τ, at constant detuning. Such a plot, displayed in Fig. 2 for $\delta = -4$, shows a shaded region ($E_H^- < E < E_H^+$), which corresponds to SP. We clearly see that no SP occurs for $\tau > \tau_c$. Conversely, decreasing τ below τ_c results into widening the portion of the upper branch that exhibits SP, until below $\tau = 1$ the whole upper branch above the switch-on threshold E_H^- turns out to be unstable. In this case, the SP switch-off energy E_H^+ diverges as the asymptote $\tau = 1$ (dashed vertical line) is approached. Importantly, for $\tau \to 0$ also the first threshold E_H^- diverges, which means that a finite response time is a key ingredient for SP to be observable. This is consistent with the fact that Kerr instantaneous nonlinearities yield no SP at all. In fact, in this case, the eigenvalues are easily found to be

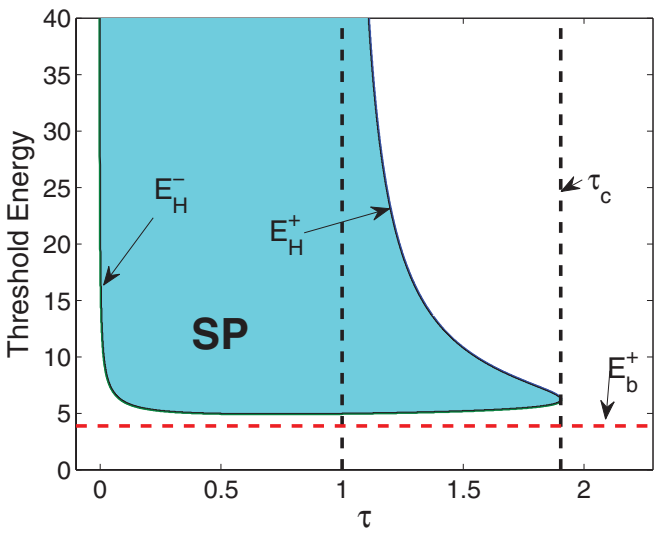

FIG. 2. (Color online) SP threshold energies $E_H^{\pm}$ as a function of τ for fixed detuning $\delta = -4$. The shaded area corresponds to the domain $E_H^- \leqslant E \leqslant E_H^+$ where SP occurs, which lies above the upper knee level of energy E_b^+ (red dashed line).

$\lambda^{\pm} = -1 \pm \sqrt{E^2 - (\delta + 2\chi E)^2}$, which rule out the possibility to have a complex-conjugate pair with a positive real part.

In order to have a complete picture and further show how the onset of SP changes with detuning, we have drawn in Fig. 3 a color map of the level curves of SP threshold energies $E_H^{\pm}$, in the parameter plane (τ,δ). A number of interesting observations can be drawn. The SP region is bounded by the border $\tau = \tau_c$, and in the bistable region ($\delta < \delta_b$) τ_c decreases with decreasing values of absolute detuning $|\delta|$. Interestingly enough, the scenario illustrated in Fig. 2 remains valid also

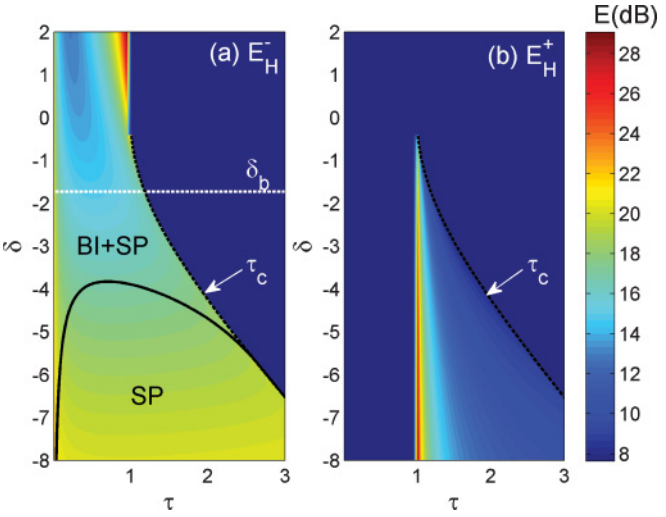

FIG. 3. (Color online) Color level plots of the (a) "on" E_H^- and (b) "off" E_H^+ values of threshold energy for SP, in the parameter plane (τ,δ). Bistability occurs below the line $\delta = \delta_b$. The curve $P(E_H^-) = P(E_b^-)$ (black solid) divides the bistable region into a domain labeled BI + SP, where SP sets in only for powers above the bistable knee for up-switching, and a domain labeled SP, where stable up-switching is not possible, being hampered by SP, which dominates the dynamics.

for detunings $\delta > \delta_b$, where bistability disappears. Finally, in the region of positive detunings, we are left with the upper branch being fully unstable for all energies $E > E_H^-$. In this region, the threshold energy E_H^- diverges, not only in the instantaneous limit $\tau = 0$, but also for $\tau = 1$, whereas relatively low values of E_H^- are found for $\tau \sim 1/2$, i.e., when the response time of the nonlinearity is nearly equal to the photon lifetime. Furthermore, the bistable region is divided into two distinct domains by the (solid black) curve which arises from the condition $P(E_H^-) = P(E_b^-)$ (its explicit expression is too cumbersome). In the domain BI + SP above such curve (bounded from above also by the line $\delta = \delta_b$), we see that the cavity can work as a bistable switch since the upper branch right above the knee for up-switching is stable [as in Figs. 1(a) and 1(c)], whereas, in the domain labeled SP below the curve, up-switching is no longer allowed, since the upper branch above the knee is SP-unstable [as shown in Figs. 1(b) and 1(d)]. The reader can easily recognize a qualitative similarity of the picture discussed here with the dynamics of SP ruled by free-carrier dispersion, recently discussed in Ref. [13]. Although a detailed analytic investigation of the stability of the SP-oscillating state (the limit cycle) is beyond the scope of this paper, similarly to the case discussed in Ref. [13], our numerical simulations of Eqs. (1) suggest that stable limit cycles, working as attractors from a large basin, exist in a wide domain of the parameter plane (witnessing the supercritical nature of the Hopf bifurcation). An example of such stable dynamics is shown in Fig. 4.

Let us comment on the observability of the SP dynamics. In nanocavities with high Q ($Q = 10^3 - 10^5$) the photon lifetime in the near infrared ranges from a few picoseconds to tens of picoseconds. While the constraint to have a response time of the nonlinearity of the same order of magnitude is naturally met in semiconductors with nonlinear response dominated by free-carrier dispersion, the same constraint in the framework of the Kerr model rules out the possibility to observe SP dynamics in media with nonlinearities of electronic origin since they are too fast (femtosecond range). Nevertheless the predictions of our Kerr model become interesting for Kerr-like materials with response time in the picosecond (ps) range, such as, e.g., soft matter, metal films [26], or more traditional liquids with reorientational nonlinearity, which are still the object of recent studies [27,28]. In particular, for instance, highly nonlinear liquids such as nitrobenzene [29] or CS_2 could be easily employed to fill a photonic crystal matrix (as also recently proposed for microstructured fibers [28]), while metal films could be employed in conjunction with dielectrics to form a single cavity or cavity arrays [30]. Assuming, for instance, a response time $\tau_{\rm phys} \sim 30$ ps [29], which yields $\tau = (\tau_{\rm phys}/2t_c) \sim 0.75$ in a cavity with $Q \sim 25\,000$ ($t_c \sim 20$ ps at $\lambda = 1.55\ \mu$m), assuming $n_{2I} \sim 10^{-17}$ m^2/W and a nonlinear modal volume $V = 3(\lambda/n)^3$, the threshold power $P = 10$ in Fig. 4 corresponds to a real-world power $P_{\rm in} = (\gamma/\Gamma_0^2)P \sim 10$ mW in the waveguide coupled to the nanocavity, where $\gamma = \omega_0 n_{2I} c/(n_{\rm eff} n V)$ is the overall nonlinear coefficient [24]. Here we have assumed a refractive index $n \sim n_{\rm eff} \sim 1.5$ and Q to be essentially determined by the coupling itself.

Having characterized so far the threshold for SP and its competition with bistability, since Ikeda and Akimoto have shown that the limit cycles destabilize, leading eventually to chaos [2], in the next section we deepen this point with the aim of determining the domain of the parameter plane where the transition to chaos could be observed.

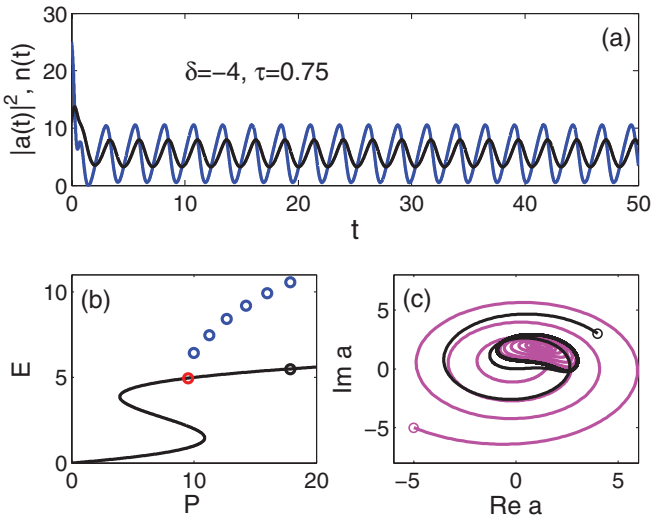

FIG. 4. (Color online) Dynamics of SP ruled by Eqs. (1), with $\delta = -4$ and $\tau = 0.75$. (a) Temporal evolution of the intracavity energy and carrier density corresponding to the rightmost blue circle in (b). (b) Steady response with superimposed peak energy of the periodic oscillations (blue open circles). The red filled circle marks the Hopf bifurcation point. The black filled circle marks the SP-unstable steady state which gives rise to the dynamics shown in (a) and (c). (c) Phase-space picture of the optical field showing the attracting limit cycle from two different initial conditions (open circles).

III. THE TURBULENT REGIME

In Ref. [2] Ikeda and Akimoto have studied the transition to chaos, identifying a period-doubling cascade up to 2^2P (i.e., oscillation with period four) at a fixed value of detuning. Here we report further details about the emergence of chaos in a wide domain of parameters. We employ different tools, ranging from the Poicaré section and its corresponding bifurcation diagram to the calculation of Lyapunov exponents. Our principal purpose is to assess whether a nanocavity described by the model Eqs. (1) can work as a reliable bistable switch and hence whether the onset of chaos should be expected when the cavity operates progressively off-resonance, especially in the region labeled BI + SP in Fig. 3. To begin with, it is instructive to report about the dynamics ruled by Eqs. (1) when, starting above the threshold P_H^-, the input power P is adiabatically decreased. In fact, this is the situation where the onset of chaos is expected according to Ref. [2]. We start at moderately low detuning ($\delta = -4$) and for $\tau = 0.45$, which corresponds to SP being unbounded on the upper branch. As shown in Fig. 5(a), in this case, the Hopf bifurcation is clearly supercritical, since the system settles on a limit cycle, whose amplitude vanishes approaching the bifurcation point [approximately as $(E - E_H^-)^{1/2}$]. However, at larger (in modulus) detunings, we observe a jump in $|a|^2$ as the limit cycle [period one ($1P$)] loses its stability and the system settles on a period-two ($2P$) oscillation, as shown in Fig. 5(b) for $\delta = -10$. The $2P$ solution does not visit anymore the simplest 1P limit cycle. Conversely

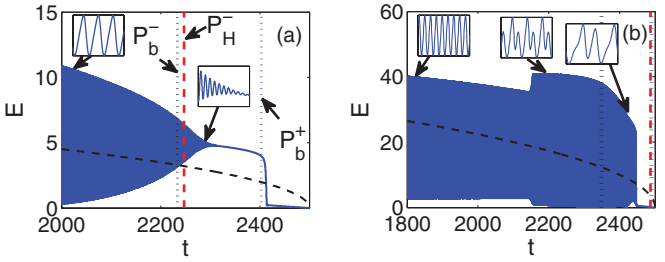

FIG. 5. (Color online) Dynamical evolution ruled by Eqs. (1) as the forcing term $\sqrt{P}$ varies adiabatically in time (dashed line). Here $\tau = 0.45$, and (a) $\delta = -4$ and (b) $\delta = -10$. The vertical lines mark the time instants at which the input power crosses the main bifurcation points: bistable knees $P_b^{\pm}$ (dotted blue and black, respectively) and Hopf threshold P_H^- (dashed red). The insets show close-up views of characteristic time intervals, indicated by arrows. Notice that in (b) the two thresholds $P_b^{\pm}$ and P_H^- almost overlap.

it abruptly switches to the stable low-branch steady state. Remarkably this happens still above the Hopf bifurcation point E_H^-. A more complex sequence of period-doubling bifurcations and chaotic motion is detected at higher detunings when the input power approaches the knee value P_b^-. In Fig. 6, where $\delta = -15$, oscillations with several different periods are evident. Moreover a chaotic regime appears, in the range $\sqrt{P} \approx 17-20$ ($P \approx 280-400$). In phase space this corresponds to the appearance of a strange attractor (not shown because its structure is already illustrated in Ref. [2]).

Since following simply the adiabatic dynamics could be possibly misleading (e.g., because of critical slowing down), as it neglects the rich variety of phenomena that occurs over the small scale, we have drawn also bifurcation diagrams calculated by collecting trajectory points on a Poincaré section for different powers. A typical example, using the same parameters as in Fig. 6, and defining the Poincaré section on the fixed phase $\angle a - \pi = 0$ of the intracavity field, is reported in Fig. 7. We can clearly identify a period-doubling cascade (up to $2^3 P$), as well as chaotic regimes. The onset of chaos follows

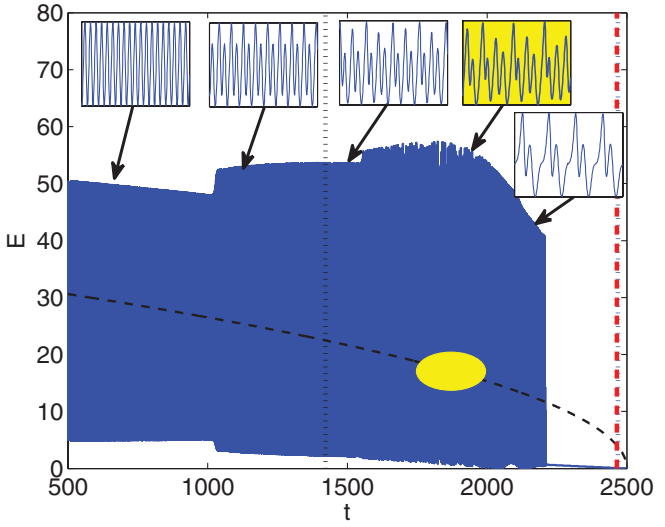

FIG. 6. (Color online) As in Fig. 5, with $\delta = -15$. The chaotic region is highlighted in yellow.

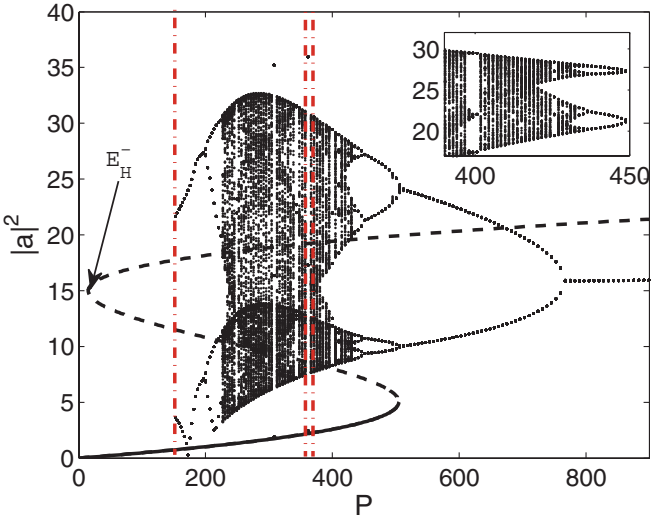

FIG. 7. (Color online) Bifurcation diagram, $\tau = 0.45$ and $\delta = -15$. The vertical dashed lines highlight a $3P$ window and the collapse at small P. Inset shows a detail in which period doubling and periodic windows can be identified more clearly.

a nontrivial scenario where narrow windows of period-three ($3P$) solutions are interspersed between two ranges of powers where the motion turns out to be chaotic. The vertical dashed lines in Fig. 7 mark indeed a $3P$ window. This is analogous to the Feigenbaum's route to chaos and confirms the observation of chaos for $P \approx 220 - 380$, already drawn above from Fig. 6.

The bifurcation diagram is computed up to $P \approx 150$ because lower power levels do not result in any limit cycle. Vice versa, the solution is observed to collapse toward the stable node represented by the lower branch of the bistable response. This phenomenon is independent from chaos, as mentioned above with reference to detuning $\delta = -10$. It occurs at large negative detunings for input powers above the SP threshold ($P > P_H^-$). This can be qualitatively explained by the coexistence of a stable fixed point (lower branch solution), a saddle (negative-slope branch), and an unstable limit cycle. As the $2P$ limit cycle spans the phase space with wide oscillations around the upper branch, it can approach the saddle point (which near the first bistable knee is closer in phase space to the center of the oscillations) being forced away, until eventually it can be captured by the lowest energy (stable) solution.

While the bifurcation map is a useful visual tool to characterize the onset to chaos and the full dynamics at fixed parameters, in order to explore in which region of the parameters one should expect to observe the chaotic dynamics, we have resorted to computing the dominant (maximal) Lyapunov exponent. We have explored a wide region of the parameter plane (τ,δ), where, in each point of such a plane, we have iterated over the values of power P to find the largest exponent. We recall that a positive Lyapunov exponent (within numerical inaccuracies) entails that the system exhibits a chaotic behavior [here quasiperiodic motion is excluded by the dissipative character of our model Eq. (1a)]. From the map displayed in Fig. 8, we notice that chaotic motion manifests itself only when the cavity is detuned far off-resonance (i.e., at very large values of $|\delta|$), provided that the SP-unstable range is not finite, or in other words that the Hopf bifurcation is

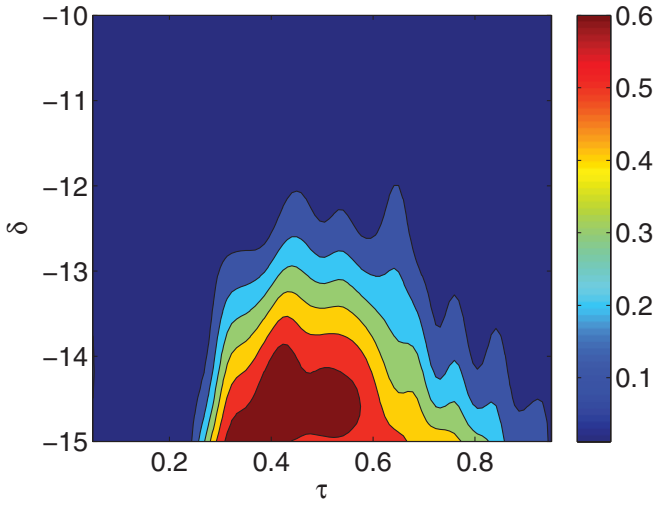

FIG. 8. (Color online) Color level map of the maximal Lyapunov exponent in the parameter plane (τ,δ).

not bounded from above ($E_H^+ \to \infty$) which requires $\tau < 1$. Therefore we can draw the important conclusion that the region where the cavity could work as a bistable switch is mutually exclusive with chaos. Therefore the onset of chaos cannot spoil the behavior of the cavity as a switch, once the latter is used in the region labeled BI + SP in Fig. 3. We point out that, in terms of power, the observation of chaos is much more challenging than stable SP since power levels leading to the former turn out to be much larger than those leading to the latter; indeed, at very large detuning, which corresponds to several times the cavity linewidth, bistability is observed at a much higher power level (compare the horizontal axis scale in Figs. 4 and 7).

As a final remark about the existence of $2^n P$ periodic solutions, we point out that they can be detected only when $P_H^- < P_b^-$ [as in the examples shown in Figs. 1(b) and 1(d)]. As discussed with reference to Figs. 1–3, this may occur not only for $\tau < 1$ (as shown explicitly above) but also for $\tau > 1$, where the Hopf bifurcation is bounded from above. More specifically $2P$ solutions are easily seen in a small subset of the region marked as SP in Fig. 3. In this case two unstable solutions, namely a repulsive (negative slope) branch and a SP branch, coexist. This seems to be a key ingredient for the limit cycles to lose their stability.

IV. CONCLUSIONS

In this work we have revisited the model that rules the behavior a passive *small* cavity with Kerr delayed response, pioneered in Ref. [2]. We have reported a full characterization of SP instabilities and their competition with bistability, outlining the existence of different possible scenarios. Importantly we have found a maximal critical value for the relaxation time that allows SP to occur and have shown that SP can have two bifurcation points, while it can occur also in the absence of bistability. We have further characterized the destabilization mechanism of the limit cycle in the full parameter space, finding that chaos is mutually exclusive with the domain where the cavity can be employed as a bistable switching element. In particular the chaotic regime predicted by Ikeda and Akimoto [2] in this system corresponds to strongly off-resonance operation, in turn implying the use of extremely high powers, thus making its observation rather challenging. Vice versa, in contrast with Kerr instantaneous nonlinearities, the observation of stable SP appears feasible in high-Q nanocavities filled with Kerr-like media with response time in the range of picoseconds. Future work will be devoted to studying the effect of coupled cavity systems and the interplay of different nonlinear mechanisms.

ACKNOWLEDGMENTS

This work was supported by the European Commission, in the framework of the Copernicus project (No. 249012).

[1] K. Ikeda, Opt. Commun. **30**, 257 (1979); K. Ikeda, H. Daido, and O. Akimoto, Phys. Rev. Lett. **45**, 709 (1980).
[2] K. Ikeda and O. Akimoto, Phys. Rev. Lett. **48**, 617 (1982).
[3] L. A. Lugiato, L. M. Narducci, D. K. Bandy, and C. A. Pennise, Opt. Commun. **43**, 281 (1982).
[4] C. M. Savage and D. F. Walls, Opt. Acta **30**, 557 (1983).
[5] L. A. Lugiato, C. Oldano, C. Fabre, E. Giacobino, and R. J. Horowicz, Il Nuovo Cimento D **10**, 959 (1988).
[6] S. Trillo and M. Haelterman, Opt. Lett. **21**, 1114 (1996); in *Spatial Solitons*, edited by S. Trillo and W. Torruellas (Springer, Berlin, 2001).
[7] H. G. Winful and G. D. Cooperman, Appl. Phys. Lett. **40**, 298 (1982).
[8] A. Parini, G. Bellanca, S. Trillo, M. Conforti, A. Locatelli, and C. De Angelis, J. Opt. Soc. Am. B **24**, 2229 (2007).
[9] G. D'Alessandro, P. St. J. Russell, and A. A. Wheeler, Phys. Rev. A **55**, 3211 (1997).
[10] M. Conforti, A. Locatelli, C. De Angelis, A. Parini, G. Bellanca, and S. Trillo, J. Opt. Soc. Am. B **22**, 2178 (2005).
[11] B. Maes, M. Fiers, and P. Bienstman, Phys. Rev. A **80**, 033805 (2009).
[12] V. Grigoriev and F. Biancalana, Phys. Rev. A **83**, 043816 (2011).
[13] S. Malaguti, G. Bellanca, A. de Rossi, S. Combrié, and S. Trillo, Phys. Rev. A **83**, 051802(R) (2011).
[14] L. A. Lugiato and R. Lefever, Phys. Rev. Lett. **58**, 2209 (1987).
[15] H. M. Gibbs, F. A. Hopf, D. L. Kaplan, and R. L. Shoemaker, Phys. Rev. Lett. **46**, 474 (1981); L. A. Orozco, A. T. Rosenberger, and H. J. Kimble, *ibid.* **53**, 2547 (1984); B. Segard and B. Macke, *ibid.* **60**, 412 (1988).
[16] K. J. Vahala, Nature (London) **424**, 839 (2003).
[17] M. Soljacic, M. Ibanescu, S. G. Johnson, Y. Fink, and J. D. Joannopoulos, Phys. Rev. E **66**, 055601(R) (2002).
[18] P. E. Barclay, K. Srinivasan, and O. Painter, Opt. Express **13**, 801 (2005).

[19] M. Notomi, A. Shinya, S. Mitsugi, G. Kira, E. Kuramochi, and T. Tanabe, Opt. Express **13**, 2678 (2005).
[20] T. Uesugi, B.-S. Song, T. Asano, and S. Noda, Opt. Express **14**, 377 (2006).
[21] E. Weidner, S. Combrié, A. de Rossi, N. V. Q. Tran, S. Cassette, A. Talneau, and H. Benisty, Appl. Phys. Lett. **89**, 221104 (2006).
[22] E. Weidner, S. Combrié, A. de Rossi, N. V. Q. Tran, and S. Cassette, Appl. Phys. Lett. **90**, 101118 (2007).
[23] S. Combrié, N. V. Q. Tran, A. de Rossi, and H. Benisty, Opt. Lett. **33**, 1908 (2008).
[24] A. de Rossi, M. Lauritano, S. Combrié, N. V. Q. Tran, and C. Husko, Phys. Rev. A **79**, 043818 (2009).
[25] X. Yang, C. Husko, C. W. Wong, M. Yu, and D. L. Kwong, Appl. Phys. Lett. **91**, 051113 (2007).
[26] M. Conforti and G. Della Valle, e-print arXiv:1109.5875v1 [physics.optics].
[27] G. Fanjoux, J. Michaud, H. Maillotte, and T. Sylvestre, Phys. Rev. Lett. **100**, 013908 (2008).
[28] C. Conti, M. A. Schmidt, P. St. J. Russell, and F. Biancalana, Phys. Rev. Lett. **105**, 263902 (2010).
[29] M. A. Duguay and J. W. Hansen, Appl. Phys. Lett. **15**, 192 (1969).
[30] R. S. Bennink, Y.-K. Yoon, R. W. Boyd, and J. E. Sipe, Opt. Lett. **24**, 1416 (1999).